

THE STARSPOTS - TRANSIT DEPTH RELATION OF THE EVAPORATING PLANET CANDIDATE KIC 12557548B

HAJIME KAWAHARA¹, TERUYUKI HIRANO², KENJI KUROSAKI¹, YUICHI ITO^{1,2}, AND MASAHIRO IKOMA¹

ABSTRACT

Violent variation of transit depths and an ingress-egress asymmetry of the transit light curve discovered in KIC 12557548 have been interpreted as evidences of a catastrophic evaporation of atmosphere with dust ($\dot{M}_p \gtrsim 1M_\oplus/\text{Gyr}$) from a close-in small planet. To explore what drives the anomalous atmospheric escape, we perform time-series analysis of the transit depth variation of Kepler archival data in ~ 3.5 years. We find that a $\sim 30\%$ periodic variation of the transit depth with $P_1 = 22.83 \pm 0.21$ days, which is within the error of the rotation period of the host star estimated using the light curve modulation, $P_{\text{rot}} = 22.91 \pm 0.24$ days. We interpret the results as an evidence that the atmospheric escape of KIC 12557548b correlates with the stellar activity. We consider possible scenarios that account for both the mass loss rate and the correlation with the stellar activity. The XUV-driven evaporation is marginally acceptable if one accepts relatively high XUV flux and high efficiency for converting the input energy to the kinetic energy of the atmosphere. Star-planet magnetic interaction is another possible scenario though huge uncertainty remains for the mass loss rate.

Subject headings: planet-star interactions– planets and satellites: atmospheres – methods: observational

1. INTRODUCTION

Planetary evaporation is one of the most crucial factors that determines the evolution and fate of close-in planets. Atmospheric escape of hot Jupiters has been extensively investigated from both the EUV observations (e.g. Vidal-Madjar et al. 2003, 2004; Lecavelier Des Etangs et al. 2010; Ehrenreich et al. 2012) and theory (e.g. Lammer et al. 2003; Baraffe et al. 2004; Yelle 2004; Lecavelier des Etangs et al. 2004; Erkaev et al. 2007; García Muñoz 2007; Murray-Clay et al. 2009). Impacts of the evaporation on the evolution of even smaller planets, including super Earths and super Neptunes, has been also recognized (e.g. Valencia et al. 2010; Owen & Jackson 2012; Lopez et al. 2012; Owen & Wu 2013; Kurosaki et al. 2013). Recently Rappaport et al. (2012) (hereafter R12) found violent variation of transit depths and an ingress-egress asymmetry of KIC 12557548, which have been interpreted as evidences of a catastrophic evaporation of a small planet (R12, Perez-Becker & Chiang 2013, hereafter PC13). Analyzing the intensity of forward scattering, Brogi et al. (2012) and Budaj (2012) found that the dust expected as an occulter of KIC 12557548 is consistent with sub-micron grains. R12 and PC13 estimated the mass loss rate of KIC 12557548b, as $\dot{M}_p \gtrsim 1M_\oplus/\text{Gyr}$.

However, a dominant energy source of the enormous evaporation remains unknown. One proposed possible scenario is that high bolometric energy input at semi-major axis $a = 0.013$ AU itself produces the hydrodynamic escape. PC13 have constructed a radiative-hydrodynamic model of KIC 12557548b assuming a Parker-type wind driven by hot planetary surface with

the equilibrium temperature ~ 2000 K. They concluded that a planet having mass $M_p \lesssim 0.02M_\oplus$ can account for the mass loss rate of KIC 12557548b. The hydrodynamic escape driven by X-ray and UV (XUV) radiations as being discussed for hot Jupiters is another candidate of the energy source. However, an XUV observation of the transit is impossible for KIC 12557548 with current satellites due to its distance.

Instead, we focus on the time-series of the transit depth. In this paper, we reanalyze the *Kepler* data of KIC 12557548, but for longer period ~ 3.5 yr than that analyzed by R12. We will find the correlation between the transit depth and the modulation of the light curve by starspots. These results indicate that the evaporation of KIC 12557548b results from some energy related to the stellar activity, rather than the bolometric one.

2. ANALYSIS OF DEPTH VARIATION

We analyze archived long cadence data of KIC 12557548 between quarter 1 and 15 (Q1-Q15; in ~ 3.5 years) using the *PyKE* package to process the data (Still & Barclay 2012). Figure 1 shows the contended long time cadence data of KIC 12557548 (Panel A) and the flattened light curve (Panel B), extracted by *kepcotrend* and *kepflatten*. Time series of the transit depth is obtained by averaging three bins ($=1.47$ hour) around central time of transit. We adopt the central time as $t_n = nP_{\text{orb}} + \text{offset}$, where $P_{\text{orb}} = 0.653558$ days (R12) and $\text{offset} = 2454900.352921$ days. Our definition of the transit depth is the average of the 3 bins of the flattened light curve, as shown by red points in Panel B of Figure 1. As shown in Panel C of Figure 1, the distribution of the flattened light curve after removal of the transit periods is well fitted by a normal distribution, at least for the lower side, which verifies that our extraction method could extract almost all of the transit periods. Figure 2 shows the time series of the extracted transit depth (top) with the cotrended light curve of the star (bottom).

kawahara@eps.s.u-tokyo.ac.jp

¹ Department of Earth and Planetary Science, The University of Tokyo, Tokyo 113-0033, Japan² Department of Earth and Planetary Sciences, Tokyo Institute of Technology, Tokyo 152-8550, Japan

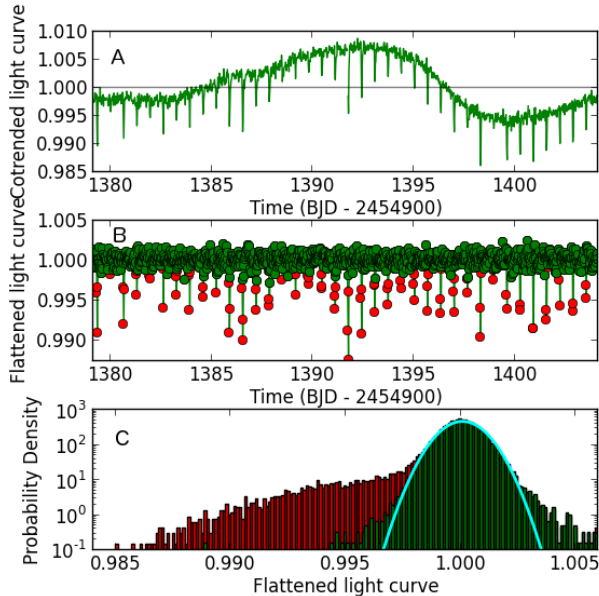


Figure 1. Panel A: a part of the contended light curve of long time cadence of KIC 12557548. Panel B: flattened light curve and identified periods (red points) of the transits. Panel C: Frequency distribution of the flattened light curve. The red tail corresponds to the transits detected by our method. The rest green is well fitted by a normal distribution (cyan).

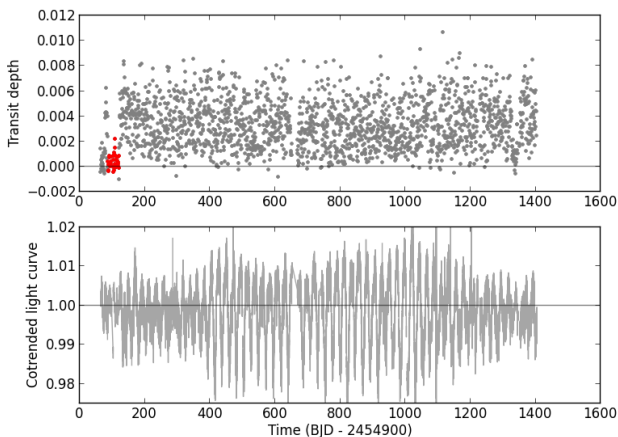


Figure 2. Transit depth variation (top) with contended light curve (bottom).

2.1. Periodicity of Transit Depth

Figure 3 shows Lomb-Scargle periodogram of the time series of the transit depth. We find three peaks above false alarm probability (FAP) = 0.1 %, $P_1 = 22.83 \pm 0.21$ days, $P_2 = 112.1 \pm 3.0$ days, and $P_3 = 152 \pm 7$ days, corresponding to FAP = 0.04 %, 10^{-5} %, and 6×10^{-4} %. We also compute periodogram of the contended light curve excluding the detected transit duration (the bottom panel in Figure 3). We find the most prominent peak at $P_{\text{rot}} = 22.91 \pm 0.24$ days and its harmonic peaks.

We also performed a high resolution spectroscopy for KIC 12557548 with High Dispersion Spectrograph on the Subaru telescope. We adopted the standard “Ra” setup with the image slicer No.2 ($R \sim 80,000$ and $510 - 780$

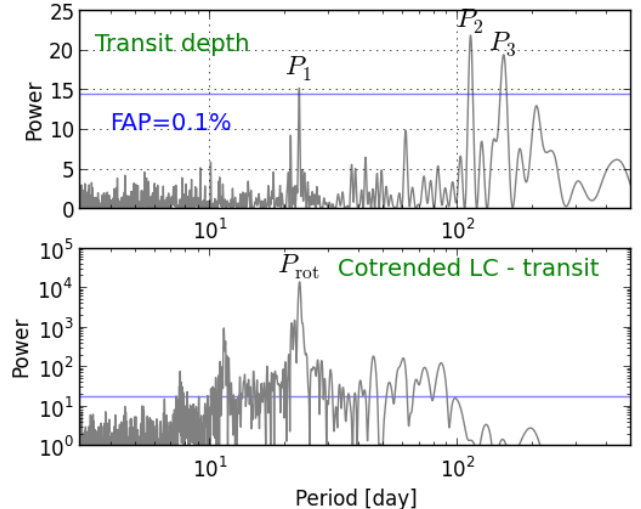


Figure 3. Lomb-Scargle periodograms of the depth variation (top) and contended light curve without transit duration (bottom). The vertical lines indicate the 0.1 % level of the FAP.

nm). The basic spectroscopic parameters were extracted based on Takeda et al. (2002) and Hirano et al. (2012): $T_{\text{eff}} = 4950 \pm 70$ K, $\log g = 3.9 \pm 0.2$, $[Fe/H] = 0.09 \pm 0.09$, and $v \sin i = 1 \pm 1$ km s $^{-1}$. The resultant systematic error in $v \sin i$ is quite uncertain because of the faintness of the target star ($V \sim 16$), but we can safely rule out a large rotational velocity, $v \sin i \gtrsim 4$ km s $^{-1}$, corresponding to a rapid rotation $P_{\text{rot}} \lesssim 8$ days (we assume $R_{\star} = 0.65 R_{\odot}$; R12).

On the assumption that this value is the stellar rotation period, the shortest periodicity found in the transit depth variation $P_1 = 22.83 \pm 0.21$ days is well consistent with the stellar rotation period. We concentrate on the periodicity of P_1 through the rest of the paper.

We fold the transit depth variation with P_1 (the top and middle panels in Figure 4). The mean value of binned data has ~ 30 % variation. We also fold the contended light curve with P_1 (the bottom panel) and find that the folded contended light curve is negatively correlated with the folded depth variation. A large starspot can survive for many years (Berdyugina 2005). The 2 % variation of the folded contended light curve can be interpreted as long term variation due to a large starspot. Hence we interpret that the planet tends to make deeper occultation as facing the large starspot.

One might attribute the depth variation of P_1 to a systematic effect of analysis. In principle, the variation of the stellar flux affects the observed depth as a systematic error. Assuming that the starspots make the variation of the contended light curve, $F_{\star} - \Delta F_{\star}$, our definition of the depth $d = S/(F_{\star} - \Delta F_{\star})$ should be negatively correlated with the contended light curve, where F_{\star} and ΔF_{\star} are the stellar flux and the extinction by the spots, and S indicates the real size of the occultation. However, as shown in the middle and bottom panels in Figure 4, the amplitude of the depth variation (~ 30 %) is much larger than that of the stellar flux variation ($\Delta F/F \sim 2$ %). Hence, we conclude that the periodicity of the depth variation synchronized with the stellar rotation is not a false positive.

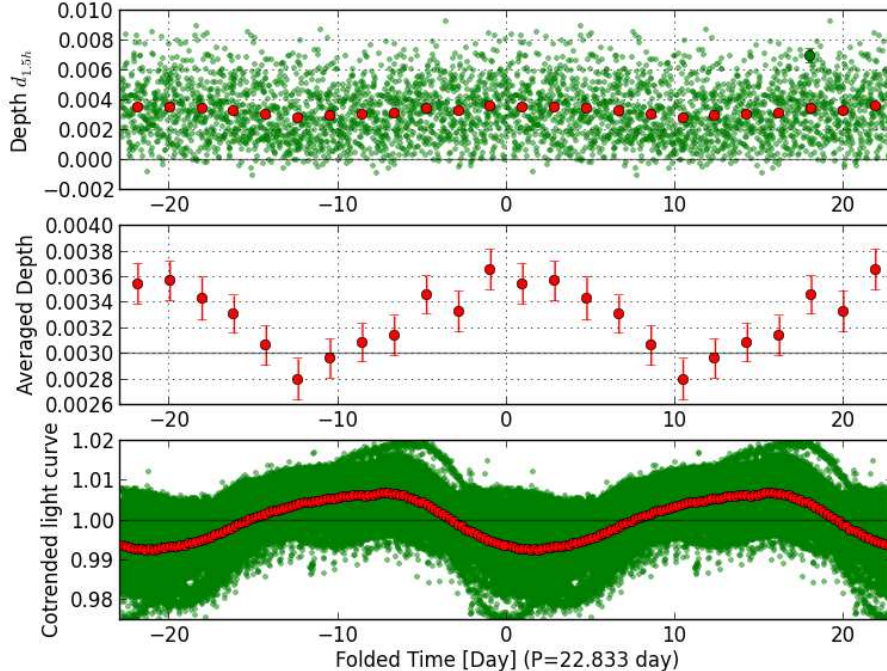


Figure 4. Top panel: the transit depth variation folded by $P_1 = 22.83 \pm 0.21$ days. A typical statistical error of the depth is shown by a green bar. Red bars are the transit depth averaged over bins. Middle panel: the mean value of the binned data of the top panel (an expanded version of the top panel around the red error bars). Bottom panel : the folded contended light curve of KIC 12557548 .

We note that Van Eylen et al. (2013) found seasonal variation of transit depth of HAT-P-7 b (i.e. $P = 365$ days) due to instrumental systematics. They did not report any other periodicity shorter than 1 year. Since the periodicity P_2 and P_3 are larger than period of a quarter, the instrumental systematics should be considered for further study.

3. INTERPRETATION

To consider possible scenarios of evaporation, two important constraints from observation, the mass-loss rate \dot{M}_p and the planet radius R_p , should be taken into account. The mass-loss rate was constrained by both R12 and PC13 in similar but slightly different ways, $\dot{M}_p \sim 1M_\oplus/\text{Gyr}$ and $\dot{M}_p > 0.1 - 1M_\oplus/\text{Gyr}$. Here we summarize the essential part of their derivation. The \dot{M}_p can be estimated using the total cross section of transit $S = \pi R_p^2 d = 7 \times 10^{19} \text{cm}^2$ (we adopt $d = 0.01$), dust density ρ_{dust} , typical length of optical path ΔL and typical time scale Δt ,

$$\begin{aligned} \dot{M}_p &\gtrsim (1 + \eta) \rho_{\text{dust}} S \Delta L / \Delta t \\ &= 1 \times (1 + \eta) \left(\frac{\rho_{\text{dust}}}{1 \text{g/cm}^3} \right) \left(\frac{\Delta L}{0.1 \mu\text{m}} \right) \left(\frac{\Delta t}{1 \text{hr}} \right)^{-1} M_\oplus / \text{Gyr} \end{aligned} \quad (1)$$

where η is the gas-dust ratio. R12 adopted $\Delta t = R_p v = 1.3$ hr, assuming the typical velocity of outflow $v = 10$ km/s, $\rho_{\text{dust}} = 3 \text{g/cm}^2$, $\Delta L = 0.2 \mu\text{m}$ as a typical grain size, which yields $\dot{M}_p \sim 1(1 + \eta)M_\oplus/\text{Gyr}$. PC13 uses an orbital period as $\Delta t = P_{\text{orb}} = 15.7$ hr, $\rho_{\text{dust}} = 1 \text{g/cm}^2$, $\Delta L = 0.5 \mu\text{m}$, which results in $\dot{M}_p \sim 0.4(1 + \eta)M_\oplus/\text{Gyr}$.

The grain size estimated from the forward scattering supported $s \sim 0.1 \mu\text{m}$ (Brogi et al. 2012; Budaj 2012).

We computed the auto correlation of the $d_{1,5h}$ and found a flat correlation for a time interval, $\tau < 10$ days. It supports $\Delta t < P_{\text{orb}}$. Assuming that the dust density is an order of g/cm^2 , we use $\dot{M}_p > 1M_\oplus/\text{Gyr}$ as a fiducial constraint of the mass loss rate.

Another constraint is the upper limit of R_p . Brogi et al. (2012) estimated the 1σ upper limit of the maximum planetary radius as $R_p < 1.2R_\oplus$ translating photometric accuracy of the phase folded light curve of no-transit-like feature (around the period marked in red in Fig. 2) into the radius.

Interpreting the starspots-depth relation in a straight forward fashion, the atmospheric escape rate should correlate with the area of the active region on the stellar surface. Because the optical flux does not change so much ($\sim 2\%$) and is negatively correlated with the transit depth, the bolometric radiation is unlikely to be a source of the relation.

3.1. XUV evaporation

Strong XUV radiation is often related to the stellar spots since the XUV flares originate from the magnetic loops. The XUV periodicity with rotation was found in a K1-type star, α centauri B (DeWarf et al. 2010) and X-ray periodicity of the F-type star was also detected (Scandariato et al. 2013). While the sunspots exhibit much smaller variation than KIC 12557548, an order-of-magnitude of variability of solar X-ray has been observed in a month (e.g. Stern 1998; Güdel 2004). We found a 6 % sudden increase of the flux during 30 minutes similar to the flare in the short cadence data. Such a strong flare will make strong XUV variation in a timescale of hours, which might account for the transit depth variation in every transit.

However, R12 questioned whether the input energy is sufficient to account for the mass loss rate. We revisit this problem using the theoretical mass-radius relation of sub/super-Earths with several different compositions. Because of lack of XUV observation, we manage to estimate the XUV flux of KIC 12557548 from the X-ray flux - rotation relation, which provides $L_X = 10^{27-28.5}$ erg/s for $P_{\text{rot}} = 23$ days (Pizzolato et al. 2003). Considering the fact that KIC 12557548 has a very large active region that makes 2 % continuous flux variation over 3.5 years, we adopt $L_{\text{XUV}}/L_{\text{solar}} = 10^{-5}$, corresponding to $L_{\text{XUV}} \sim 10^{28.5}$ erg/s.

In the energy-limit regime (Watson et al. 1981; Lammer et al. 2003; García Muñoz 2007; Lecavelier Des Etangs 2007), the mass loss rate can be estimated as

$$\dot{M}_p(R_p) = \epsilon \frac{\pi r_1^2 F_{\text{XUV}}}{GM_p/r_0} \frac{1}{K_{\text{tide}}}, \quad (2)$$

where r_0 is the radius where gas is bound to the planet, r_1 is the radius where the bulk of incoming XUV flux is absorbed, ϵ is the efficiency for converting the input energy to the kinetic energy of the atmosphere. There is controversy as to which radius should be adopted to r_1 (e.g. Baraffe et al. 2004; García Muñoz 2007; Murray-Clay et al. 2009), we adopt the radius where optical depth ~ 1 conservatively, i.e. $r_0 = r_1 = R_p$.

A correction factor of the Roche lobe effect, K_{tide} , (Erkaev et al. 2007) is given by,

$$K_{\text{tide}} = 1 - \frac{3}{2} \left(\frac{R_p}{R_H} \right) + \frac{1}{2} \left(\frac{R_p}{R_H} \right)^3, \quad (3)$$

where R_H is the Hill radius,

$$R_H \sim 3.4 \left(\frac{M_p}{M_{\oplus}} \right)^{1/3} \left(\frac{M_{\star}}{0.7M_{\odot}} \right)^{-1/3} R_{\oplus}. \quad (4)$$

On the basis of Kurosaki et al. (2013), we compute the mass-radius relation of planets composed of 100 % water, 50% water+50% rocky core, 10% water+90 % rocky core (volatile-rich planets), 100 % rock, and 100 % iron assuming the equilibrium temperature of KIC 12557548b (~ 1800 K). We neglect the contribution of thin atmosphere, which should be evaporating, for the 100 % rock and iron planets to compute the relation. The interior structure of the planet is computed with equations of the hydrostatic equilibrium, mass conservation, and energy conservation (e.g. Kippenhahn & Weigert 1990) and the equation of state (EOS). The EOS of water is based on H2O-REOS (French et al. 2009) at high pressure and the ideal gas with the effects of dissociation of H₂O developed by Hori & Ikoma (2011). The rocky core is assumed to be the same in composition as the bulk silicate Earth and the EOS of the rocky and iron cores are given by Valencia et al. (2007). We also consider the atmospheric structure for the water planets assuming the radiative equilibrium and define the radius at the point of the thermal optical depth=2/3, approximately corresponding to the visible optical depth ~ 1 .

Figure 5 (left) shows the mass-radius relation of these planets. We find that the radius of volatile-rich (the water fraction being $\gtrsim 10$ %) planets cannot be smaller

than the upper limit of planetary radius $\sim 1.2R_{\oplus}$ because the gravity cannot bind the atmosphere. Therefore a volatile-rich planet is unlikely to be KIC 12557548b. Figure 5 (right) shows \dot{M}_p expected in the energy-limit case, assuming the relatively high flux $L_{\text{XUV}} = 10^{-5}L_{\odot}$ and an optimistic assumption of the efficiency $\epsilon = 0.5$. The density of the planet composed of iron is too dense to obtain the mass loss rate needed. The \dot{M}_p of the rocky planet is $\sim 1M_{\oplus}/\text{Gyr}$. The Roche lobe effect increases \dot{M}_p by two times larger than that without the tide. R12 discussed that the XUV luminosity is at least a factor of 10 too low compared to the luminosity needed assuming $\epsilon = 0.1$. The Roche lobe effect and the assumption of ϵ are likely to make the difference by one order-of-magnitude in \dot{M}_p between R12 and us. Though our assumptions are very optimistic, the rocky planet is marginally acceptable as a candidate of KIC 12557548b.

One might consider that additional volatile components on the rocky planet increase the planetary effective radius and \dot{M}_p . To estimate this effect, we derive the surface pressure needed to increase the transit radius R_t to χ times of the radius of the silicate core R_b ($R_t = R_b + h = (1 + \chi)R_b$) though the observed transit radius is not identical to the effective radius for equation (2). We adopt $\chi = 0.5$, i.e. ~ 2 times larger cross section. The atmospheric height from the ground to the point where the optical depth through the planetary limb is unity is estimated by assuming the isothermal atmosphere with temperature T and a power-law dependence of the opacity on pressure ($\kappa \propto P^{\alpha}$; Rogers & Seager 2010),

$$h = \frac{H}{\alpha + 1} \log \left(\frac{\tau_b}{\tau(r)} \right) \quad (5)$$

where $H = kT/\mu m_H g$ is the pressure scale height, P_b , μ and m_H are the surface pressure at the lower boundary of the atmosphere, mean-molecular weight and proton mass. The vertical optical depth $\tau(r)$ is linked to the optical depth of the chord (e.g. Burrows et al. 2007; Hansen 2008; Rogers & Seager 2010) as

$$\tau_t(r) \approx \sqrt{\frac{2\pi(\alpha + 1)r}{H}} \tau(r). \quad (6)$$

It yields

$$h = \frac{H}{\alpha + 1} \log \left(\sqrt{\frac{2\pi(h + R_b)}{H(\alpha + 1)}} \frac{\kappa_b P_b}{g} \right), \quad (7)$$

where κ_b is the visible opacity at the surface. Then we obtain

$$P_b = \sqrt{\frac{\alpha + 1}{\chi + 1}} \frac{g}{\kappa_b} \frac{e^{\chi(\alpha + 1)\lambda_b}}{\sqrt{2\pi\lambda_b}} \sim 10^{0.4\chi(\alpha + 1)\lambda_b - \Delta} \left(\frac{\kappa_b}{1 \text{ cm}^2/\text{g}} \right)^{-1} [\text{bar}] \quad (8)$$

where $\lambda_b \equiv GM\mu m_H/kTR_b$ is the escape parameter and $\Delta \sim 4.5$ for $M = (0.01 - 1)M_{\oplus}$ and $\rho = 4 \text{ g/cm}^3$. For the Na atmosphere, which is a possible dominant component of the atmosphere of the rocky planets (e.g. Miguel et al. 2011), $\kappa_b \sim 10^2(P/1\text{bar})^1$ for $10^{-2} - 10^3$ bar, where we computed $\kappa_b(\lambda)$ based on Atomic Line Data (Kurucz & Bell 1995) with the

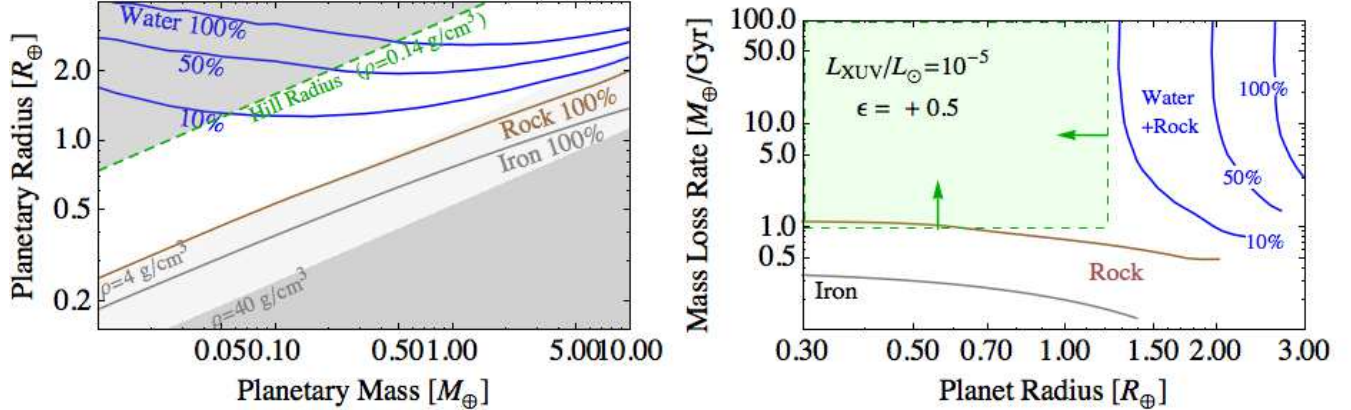


Figure 5. The mass-radius relation (left) and \dot{M}_p in the energy-limited regime assuming the XUV driven escape (right). In the left panel, a green dashed line indicates the hill radius assuming $M_* = 0.7M_\odot$ and $a = 0.013$ AU. In the right panel, fiducial constraints derived by the minimum transit depth and the mass loss estimate are shaded by green. We assume relatively high value of the XUV flux $L_{XUV} = 10^{-5} L_\odot$ and high efficiency $\epsilon = 0.5$.

method by Piskunov & Kupka (2001) and took the logarithm average of $\kappa_b(\lambda)$ (see Eq. [7]) for the Kepler band. Adopting $\mu = 30$, we obtain $P_b \sim 10$ bar and 1 bar for $M = 0.1M_\oplus$ ($\lambda_b \sim 24$) and $M = 0.01M_\oplus$ ($\lambda_b \sim 5$), which are much higher than the equilibrium vapor pressure of the olivine, $10^{-5} - 10^{-2}$ bar for 2000-2500 K (Perez-Becker & Chiang 2013) (see also Miguel et al. 2011). Thus the Na atmosphere vaporized at the equilibrium temperature is difficult to increase the effective cross section of XUV. Though we assumed the equilibrium temperature as the surface temperature for simplicity, further study of detailed properties of the atmospheric structure and the boundary condition of magma ocean is needed to derive the realistic contribution of the volatile components.

3.2. Energetic Electron by Magnetic Reconnection

Star-planet magnetic interaction is another possible scenario for a catastrophic evaporation that correlates with stellar activity. Recently Lanza (2013) proposed a new scenario that energetic electrons released by magnetic reconnection at the boundary of the planetary magnetosphere inject kinetic energy into the planetary atmosphere. The power released by the reconnection per area, corresponding flux, is estimated (Lanza 2012, 2013) as

$$F_{\text{mag}} \equiv \frac{P_{\text{mag}}}{\pi R_p^2} = \frac{B_0^2}{2\mu_B} \sqrt{\frac{GM_*}{a}} \left(\frac{B_p}{B_0}\right)^{2/3} \left(\frac{R_*}{a}\right)^{4s/3} \quad (9)$$

where μ_B is the magnetic permeability of the plasma, B_0 and B_p are the magnetic field at the pole of a star and a planet. If adopting $B_0 = 10$ G, $B_p = 1$ G, and $s = 2$, we obtain $4\pi a^2 F_{\text{mag}} = 5 \times 10^{-5} (\mu_B/\mu_0)^{-1} L_\odot$, (μ_0 is vacuum permeability). Since this value is larger than our fiducial value of $L_{XUV} = 10^{-5} L_\odot$ in §3.1, it is possible to account for the mass loss rate.

4. SUMMARY

We performed the time-series analysis of the transit depth of KIC 12557548b. We found that the transit depth variation has three values of specific periodicity above FAP=0.1 % and that the shortest one $P_1 = 22.83 \pm 0.21$ days is consistent with the stellar rotation period estimated by the light curve modulation. We

interpreted these results as an evidence that the evaporation is related to the stellar activity.

Using the theoretical mass-radius relation with tide, we show that the massive escape of a rocky planet driven by XUV is possible if assuming high XUV flux and high efficiency. We estimate the amount of the volatile components to increase the XUV cross section. Though the vapor pressure at $T \sim 2000$ K is not enough to increase \dot{M}_p , further study of the atmosphere with magma ocean is needed. The energetic electrons released by the magnetic reconnection is another possible energy to lead to the massive escape. Though we could not identify any plausible scenario to account for the $\sim 1M_\oplus/\text{yr}$ evaporation correlated with stellar activity, future XUV observations will enable us to understand what type of energy evaporates close-in small planets if future surveys of transiting planets such as *Transiting Exoplanet Survey Satellite* find nearby similar systems.

We are grateful to Yoichi Takeda, for the helpful discussion and spectroscopic analysis. This work is supported by the Astrobiology Project of the Center for Novel Science Initiatives (CNSI), National Institutes of Natural Sciences (NINS) (Grant Number AB251009) and by Grant-in-Aid for Scientific research from JSPS and from the Japanese Ministry of Education, Culture, Sports, Science and Technology (Nos. 25800106, 25400224, and 25-3183).

REFERENCES

- Baraffe, I., Selsis, F., Chabrier, G., Barman, T. S., Allard, F., Hauschildt, P. H., & Lammer, H. 2004, *A&A*, 419, L13
 Berdyugina, S. V. 2005, *Living Reviews in Solar Physics*, 2, 8
 Brogi, M., Keller, C. U., de Juan Ovelar, M., Kenworthy, M. A., de Kok, R. J., Min, M., & Snellen, I. A. G. 2012, *A&A*, 545, L5
 Budaj, J. 2012, arXiv:1208.3693
 Burrows, A., Hubeny, I., Budaj, J., & Hubbard, W. B. 2007, *ApJ*, 661, 502
 DeWarf, L. E., Datin, K. M., & Guinan, E. F. 2010, *ApJ*, 722, 343
 Ehrenreich, D., et al. 2012, *A&A*, 547, A18
 Erkaev, N. V., Kulikov, Y. N., Lammer, H., Selsis, F., Langmayr, D., Jaritz, G. F., & Biernat, H. K. 2007, *A&A*, 472, 329
 French, M., Mattsson, T. R., Nettelmann, N., & Redmer, R. 2009, *Phys. Rev. B*, 79, 054107
 García Muñoz, A. 2007, *Planet. Space Sci.*, 55, 1426
 Güdel, M. 2004, *A&A Rev.*, 12, 71

- Hansen, B. M. S. 2008, *ApJS*, 179, 484
- Hirano, T., Sanchis-Ojeda, R., Takeda, Y., Narita, N., Winn, J. N., Taruya, A., & Suto, Y. 2012, *ApJ*, 756, 66
- Hori, Y., & Ikoma, M. 2011, *MNRAS*, 416, 1419
- Kippenhahn, R., & Weigert, A. 1990, *Stellar Structure and Evolution*
- Kurosaki, K., Ikoma, M., & Hori, Y. 2013, arXiv:1307.3034
- Kurucz, R., & Bell, B. 1995, *Atomic Line Data* (R.L. Kurucz and B. Bell) Kurucz CD-ROM No. 23. Cambridge, Mass.: Smithsonian Astrophysical Observatory, 1995., 23
- Lammer, H., Selsis, F., Ribas, I., Guinan, E. F., Bauer, S. J., & Weiss, W. W. 2003, *ApJ*, 598, L121
- Lanza, A. F. 2012, *A&A*, 544, A23
- Lanza, A. F. 2013, arXiv:1307.2341
- Lecavelier Des Etangs, A. 2007, *A&A*, 461, 1185
- Lecavelier Des Etangs, A., et al. 2010, *A&A*, 514, A72
- Lecavelier des Etangs, A., Vidal-Madjar, A., McConnell, J. C., & Hébrard, G. 2004, *A&A*, 418, L1
- Lopez, E. D., Fortney, J. J., & Miller, N. 2012, *ApJ*, 761, 59
- Miguel, Y., Kaltenecker, L., Fegley, B., & Schaefer, L. 2011, *ApJ*, 742, L19
- Murray-Clay, R. A., Chiang, E. I., & Murray, N. 2009, *ApJ*, 693, 23
- Owen, J. E., & Jackson, A. P. 2012, *MNRAS*, 425, 2931
- Owen, J. E., & Wu, Y. 2013, arXiv:1303.3899
- Perez-Becker, D., & Chiang, E. 2013, *MNRAS*
- Piskunov, N., & Kupka, F. 2001, *ApJ*, 547, 1040
- Pizzolato, N., Maggio, A., Micela, G., Sciortino, S., & Ventura, P. 2003, *A&A*, 397, 147
- Rappaport, S., et al. 2012, *ApJ*, 752, 1
- Rogers, L. A., & Seager, S. 2010, *ApJ*, 712, 974
- Scandariato, G., et al. 2013, *A&A*, 552, A7
- Stern, R. A. 1998, in *Astronomical Society of the Pacific Conference Series*, Vol. 154, *Cool Stars, Stellar Systems, and the Sun*, ed. R. A. Donahue & J. A. Bookbinder, 223
- Still, M., & Barclay, T. 2012, *PyKE: Reduction and analysis of Kepler Simple Aperture Photometry data*, *Astrophysics Source Code Library*
- Takeda, Y., Ohkubo, M., & Sadakane, K. 2002, *PASJ*, 54, 451
- Valencia, D., Ikoma, M., Guillot, T., & Nettelmann, N. 2010, *A&A*, 516, A20
- Valencia, D., Sasselov, D. D., & O'Connell, R. J. 2007, *ApJ*, 656, 545
- Van Eylen, V., Lindholm Nielsen, M., Hinrup, B., Tingley, B., & Kjeldsen, H. 2013, arXiv:1307.6959
- Vidal-Madjar, A., et al. 2004, *ApJ*, 604, L69
- Vidal-Madjar, A., Lecavelier des Etangs, A., Désert, J.-M., Ballester, G. E., Ferlet, R., Hébrard, G., & Mayor, M. 2003, *Nature*, 422, 143
- Watson, A. J., Donahue, T. M., & Walker, J. C. G. 1981, *Icarus*, 48, 150
- Yelle, R. V. 2004, *Icarus*, 170, 167